

Electronic Supplementary Information

Nitrogen-doped hollow carbon spheres with wrinkled surface: one-pot carbonization synthesis and supercapacitor properties

Lei Liu,^{a*} Shi-Da Xu,^a Qing Yu,^a Feng-Yun Wang,^{b*} Hui-Ling Zhu^a, Ru-Liang Zhang^a and Xin Liu

1. Experimental section

1.1 Chemicals

Graphite was supplied by Alfa Aesar. Resorcinol, formaldehyde, melamine, citric acid, formic acid and hexamethylenetetramine (HMT) were purchased from Laiyang Fine Chemical Factory. Melamine, citric acid was purchased from Tianjin Fuchen Chemical Co. All of chemicals were of analytical grade without further purification.

1.2 Synthesis

MF spheres. In a typical synthesis, 8.494 g of 37 wt % formaldehyde solution was prepared by mixing 200 mL of distilled water. Subsequently, 2.0 g of melamine was added and stirred at 80 °C. After melamine completely dissolved, formic acid were added (pH = 5), and the mixed solution was stirred for 2 h. Finally, the solid product was obtained by centrifugation, washed several times by deionized water and pure ethanol to remove impurities and dried at 150 °C for 12 h. The resulting polymer spheres were collected and labeled as MF spheres.

GO. GO was prepared from natural graphite powder using modified Hummers method ^[1]. For purification, the product was washed several times with 5% HCl and distilled water. The product was exfoliated by ultrasonication for 2 h. Finally, a homogeneous GO aqueous suspension was

obtained and used for the further preparation of GO-resol@MF composites.

GNHCSs. 0.5 g of MFS was dispersed in a mixture of distilled water and ethanol (volume ratio 1:1) by ultrasonication, followed by adding of 1.0 mL of graphene oxide (GO) solution (0.01g GO dispersed in 20 mL water) under continuous stirring for 0.5 h, then centrifugation to give a solid product. Then, the solid product was dispersed in an aqueous-alcoholic solution by mixing ethanol and distilled water (volume ratio 1:1). After that, 1.05 g of hexamethylenetetramine and 0.8 g of resorcinol were added sequentially. And then 1.0 g of citric acid was added as catalyst and stirred for 24 h at 30 °C. Finally, 1.0 mL of GO solution was added under continuous stirring for another 0.5 h, the solid product was obtained by centrifugation and dried at 60 °C for 5 h and labeled as GNPSs. The obtained nitrogen enriched hollow carbon spheres were denoted as GNHCSs after carbonization in N₂ at 600°C for 3 h, with a heating rate of 1 °C min⁻¹. In order to investigate the effect of GO amount on the morphology of the obtained hollow carbon spheres, another two samples with different feeding amount of GO (2.0 and 3.0 mL) were also prepared, labeled as GNHCSs-1 and GNHCSs-2.

NHCSs. For comparison, NHCSs were prepared in the absence of GO solution. The other procedures were same to that for GNHCSs.

1.3 Characterization

Scanning electron microscopy (SEM) was carried out on a Nova Nano SEM450 microscope at 15 keV. Transmission electron microscopy (TEM) measurements were performed on a FEI Tecnai F20 microscope at 200 kV. All samples subjected to TEM measurements were ultrasonically dispersed in ethanol and drop-cast onto copper grids covered with carbon film. X-ray photoelectron spectroscopy (XPS) measurements were performed on a Kratos Axis Ultra

DLD (delay line detector) spectrometer equipped with a monochromatic Al K X-ray source (1486.6 eV). All XPS spectra were recorded using an aperture slot of $300\ \mu\text{m} \times 700\ \mu\text{m}$, survey spectra were recorded with a pass energy of 160 eV, and high-resolution spectra with a pass energy of 40 eV. Fourier transform infrared (FT-IR) spectra were collected on a Nicolet Fourier spectrophotometer, using KBr pellet technique. Nitrogen adsorption-desorption isotherms were measured on Quadrasorb evo at -196°C . Before measurements, the samples were degassed at 200°C for at least 6 h. The specific surface area (S_{BET}) was calculated according to the Brunauer-Emmett-Teller (BET) method ($0.01 < P/P_0 < 0.1$), the pore size distribution was derived from the adsorption branch of isotherms using non-local density functional theory (NLDFT) method, and the total pore volume (V_{total}) was estimated from the adsorbed amount at a relative pressure P/P_0 of 0.980. Micropore surface area and micropore volume were obtained via t-plot analysis. Thermogravimetric analysis (TGA) curves were recorded on a TGA/DSC1/1600LF analyzer under a constant air flow of $100\ \text{mL}\ \text{min}^{-1}$ with a temperature rate of $10\ ^\circ\text{C}\ \text{min}^{-1}$.

1.4 Electrochemical Measurements.

Electrochemical measurements were conducted with a three-electrode electrochemical cell with 6 M KOH aqueous electrolyte on CHI760E electrochemical workstation. The standard three-electrode electrochemical cell was fabricated using platinum sheet as the counter electrode, and saturated calomel electrode as the reference electrode. The working electrodes were prepared by mixing the active material, acetylene black and polytetrafluoroethylene (PTFE) binder with a weight ratio of 85: 10: 5. After coating the above slurry onto the nickel foam current collector ($1\ \text{cm} \times 1\ \text{cm}$), the electrodes were dried at 70°C overnight before pressing under a pressure of 10 MPa. The cyclic voltammetry (CV) voltage scanning range was from -1.0 to 0V , with the scan

rate from 5 to 100 mV s⁻¹. Galvanostatic charge–discharge cycling was also performed in the 0 and -1.0 V range in the aqueous medium at current densities in the 0.5–20 A g⁻¹ range based on the active mass of a single electrode. The specific gravimetric capacitance of a single electrode (Fg⁻¹) determined from the galvanostatic cycles was calculated by means of the formula:

$$C_g = \frac{I \cdot \Delta t}{m \cdot \Delta V}$$

where I , Δt , ΔV , and m are the applied current, discharge time, voltage change, and the mass of active material, respectively. The electrochemical impedance spectroscopy (EIS) was conducted at an amplitude of 10 mV in the frequency range from 100 kHz to 10 mHz on IM6 and ZENNIUM electrochemical workstation.

2. Supplementary Figures

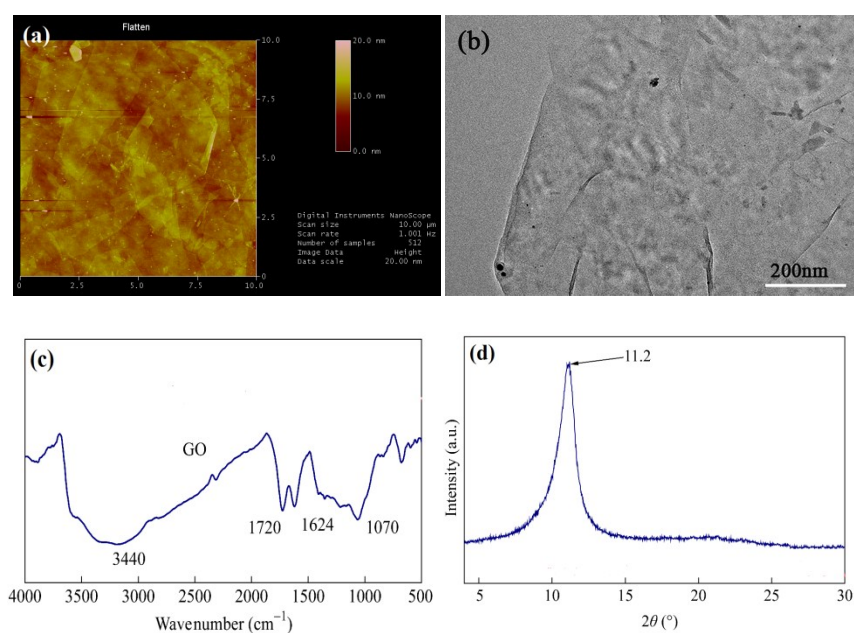


Fig. S1 AFM image (a), TEM images (b), FTIR spectra (c), and wide angle XRD patterns (d) of GO. FTIR spectra showed four major characteristic peaks including a broad peak at 3440 cm⁻¹ (O–H stretching vibration), and peaks at 1720 cm⁻¹ (C=O stretching), 1624 cm⁻¹ (C=C stretching vibration) and 1070 cm⁻¹ (C–O–C stretching in epoxy group) in GO spectrum. XRD patterns depict one characteristic peak at 11.2° of GO corresponding to the inter layer spacing of, 0.79 nm. The increase of *d* value compared to pristine graphene (0.34 nm) indicates the exfoliation of GO.

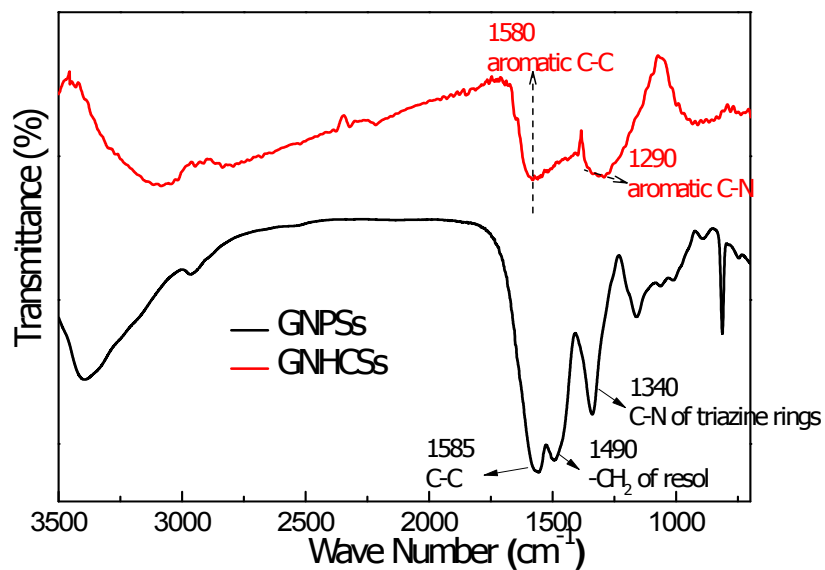


Fig. S2 FT-IR spectra of polymer and hollow carbon spheres. (a) GNPSs; (b) GNHCSs. Compared with polymer sample GNPSs, most absorption peaks of MF resins completely disappear in the curve of GNHCSs. There are only two broad new peaks at 1290 and 1585 cm^{-1} , corresponding to the vibrations of aromatic C-N bond and the aromatic ring, respectively.

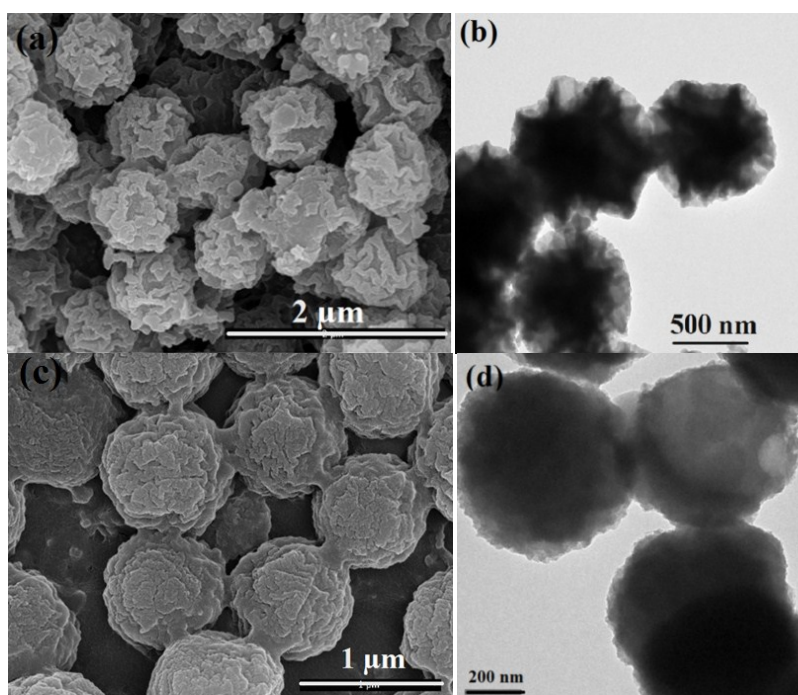


Fig. S3 SEM and TEM images of GNHCSs-1 (a, b) and GNHCSs-2 (c, d).

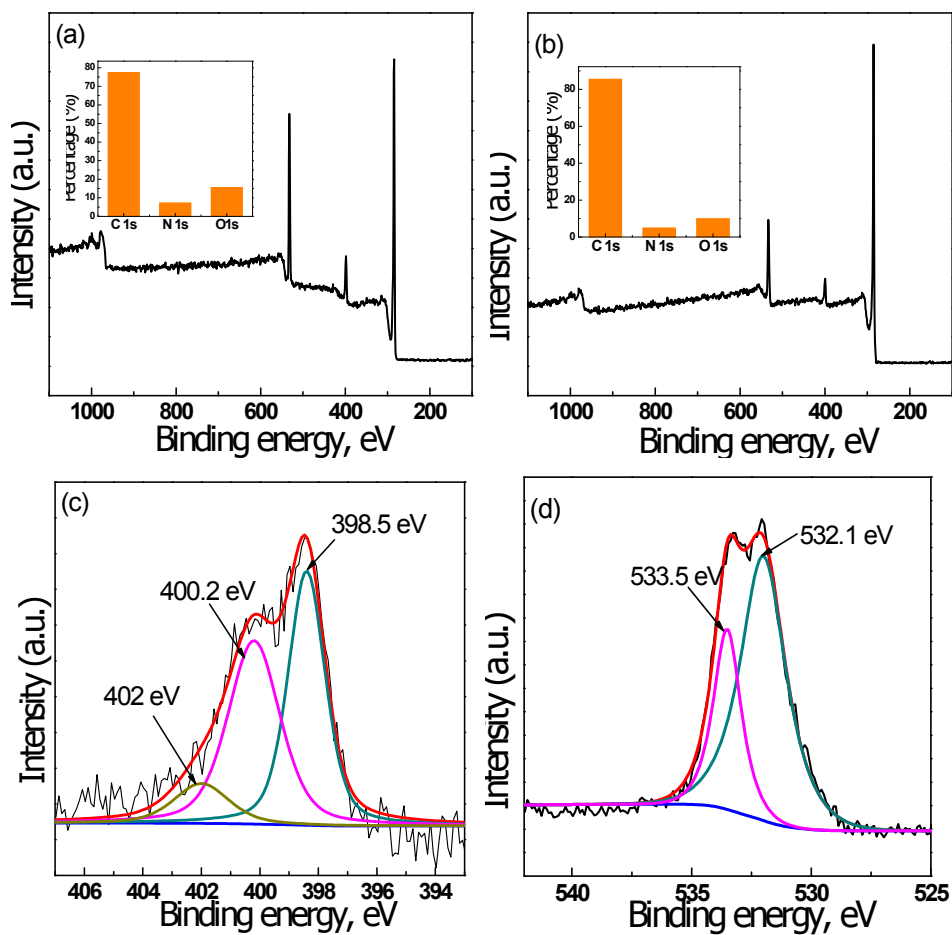


Fig. S4 XPS survey spectrum of GNHCSs (a) and NHCSs (b). The insert is the corresponding content of each element. High-resolution XPS spectra of N 1s (c), and O 1s (d) in NHCSs. It can be found that the N and O contents of NHCSs are 4.8% and 9.8%, respectively, much lower than that of GNHCSs.

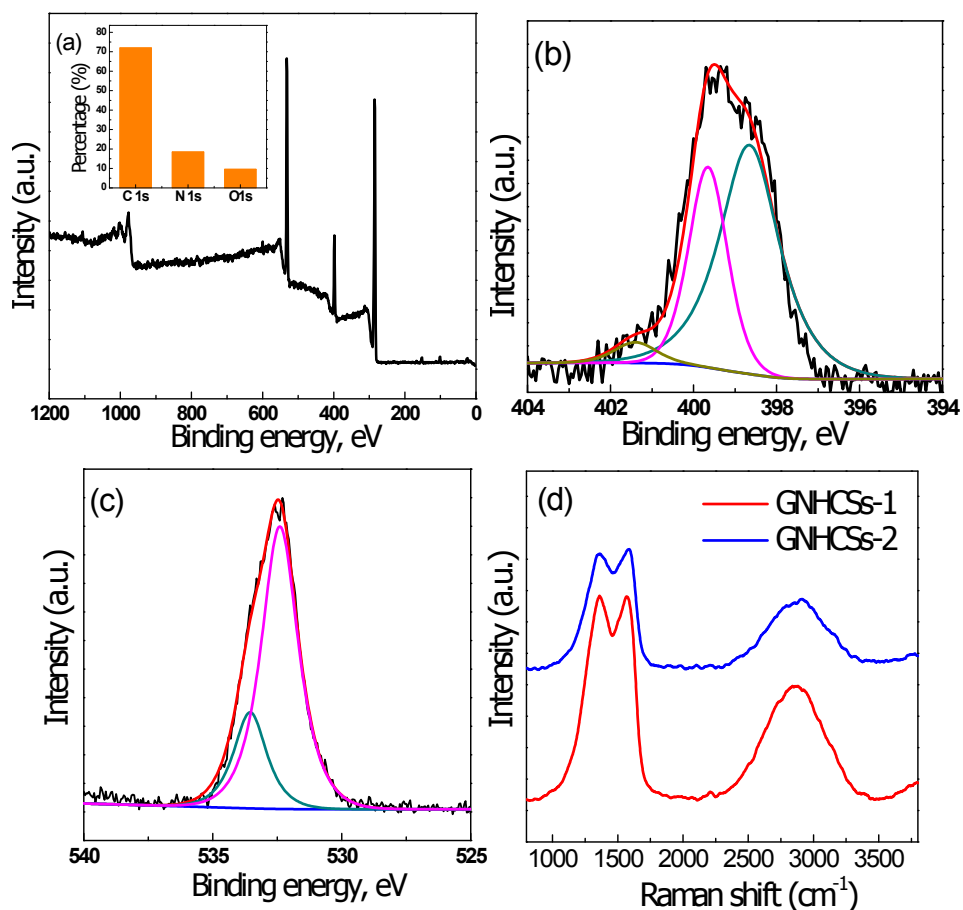


Fig. S5 XPS survey spectrum of GNHCSs-1 (a). The insert is the corresponding content of each element. High-resolution XPS spectra of N 1s (b), and O 1s (c) in GNHCSs-1. Raman spectra of GNHCSs-1 and GNHCSs-2. It can be found that the N and O contents of GNHCSs-1 are 9.6% and 18.5%, respectively. The I_D/I_G value further decreased with the increase of GO, to 0.99 and 0.97 for GNHCSs-1 and GNHCSs-2, respectively, which can be related to the modification of graphene.

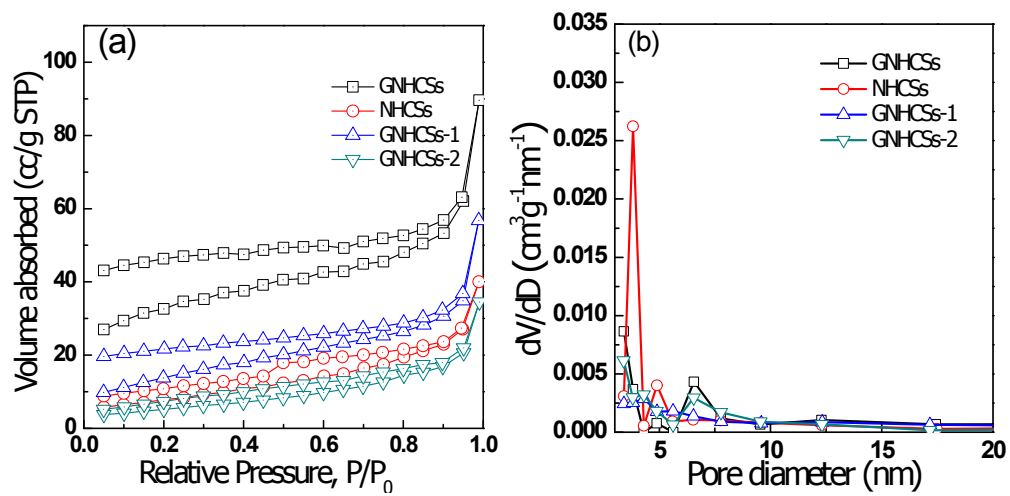


Fig. S6 (a) N_2 adsorption/desorption isotherms at 77 K and (b) pore size distribution curves of different hollow carbon spheres.

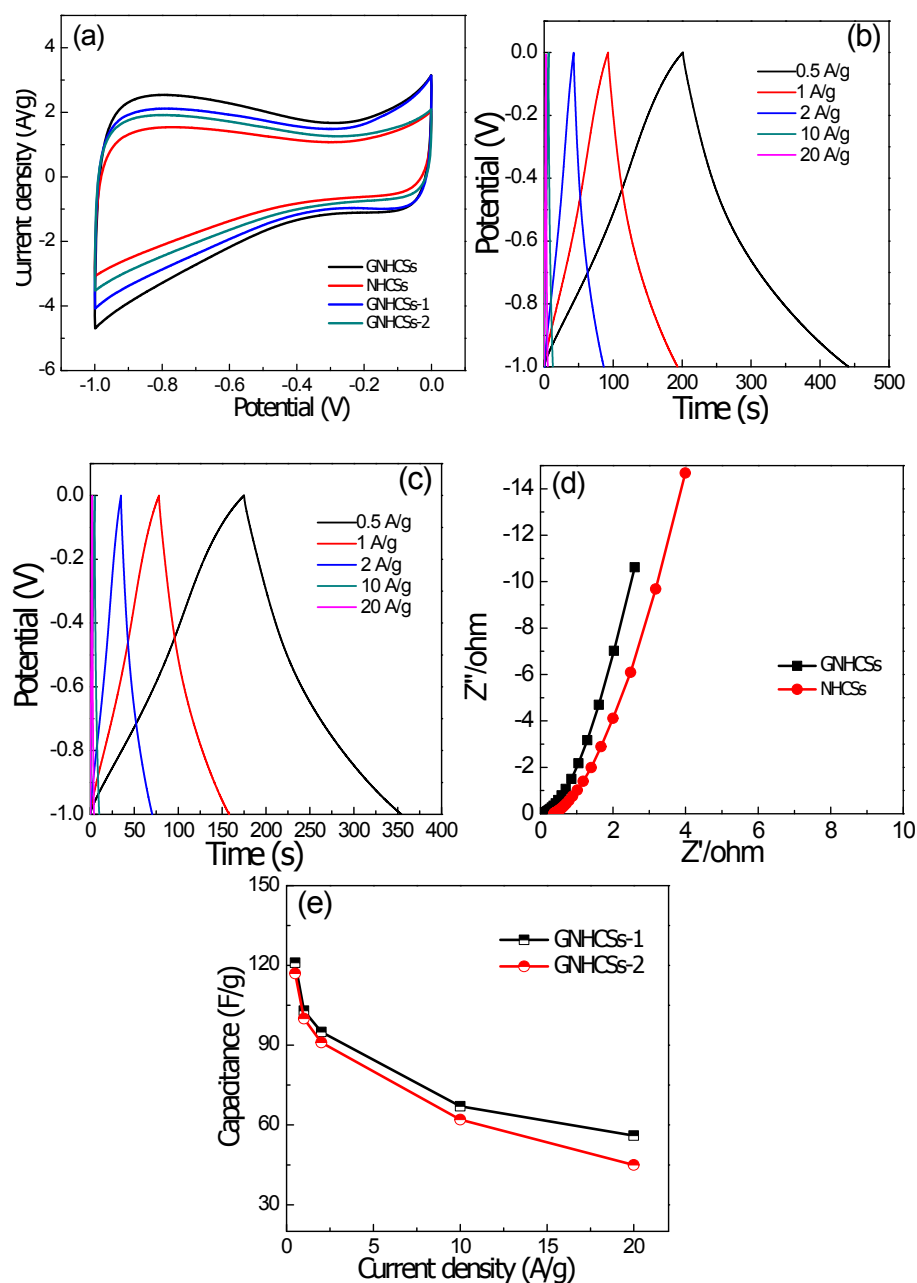


Fig. S7 CV curves of sample GNHCSs and NHCSs at scan rates of 20 mV s^{-1} in 6 M KOH solution (a). Galvanostatic charge-discharge curves of GNHCSs (b) and NHCSs (c) at different current densities (0.5-20 A/g). Electrochemical impedance spectra of GNHCSs and NHCSs (d). Specific capacitances of GNHCSs-1 and GNHCSs-2 electrodes at different current densities (0.5-20 A/g) (e). GNHCSs exhibit a low resistance ($0.12 \ \Omega$) than that of NHCSs ($0.38 \ \Omega$), indicating a higher conductivity of GNHCSs. The specific capacitance of GNHCSs-1 and GNHCSs-2 at current density of 0.5 A/g determined from the discharge process was 120 and 117

F/g, respectively. The specific capacitance of GNHCSs-1 at 20 A/g preserved capacitance retention of 46% of the value at 0.5 A g⁻¹, while GNHCSs-2 maintained 38% at the same conditions, much lower than that of GNHCSs (50%), indicating highly wrinkled surface accompanied with good rate performance.

Table S1 Comparison of capacitance data reported for different carbon-based materials.

Samples	Electrolyte	S_{BET} (m^2g^{-1})	Scan rate	Specific capacitance (F g^{-1})	Capacitance Retention	Ref.
Phenolic resin-derived carbon spheres (CS3-6)	1 M H_2SO_4	530	1 A g^{-1}	105	--	2
Carbon nanosheets from organic salt	Organic electrolyte	1400	1 mV s^{-1}	150	~94%(10000 cycles)	3
Nitrogen and oxygen doped hollow carbon spheres (HCSs-700)	6 M KOH	355	0.5 A g^{-1}	210	43% (5A/g)	4
Polyaniline-derived porous nitrogen-doped hollow carbon spheres	6 M KOH	213	0.5 A g^{-1}	213	56% (10A/g) ~91%(5000 cycles)	5
Resol resin-derived yolk-shell structured carbon nanospheres	6 M KOH	1068	10 mVs^{-1}	159	----	6
Graphene-coated hollow mesoporous carbon spheres	0.5 M NaCl	400	10 mV s^{-1}	43.2	---	7
Three-dimensional porous architectures	1 M Na_2SO_4	1260	0.58 A g^{-1}	58	~95% (4000)	8
This work	6 M KOH	124	0.5 A g^{-1}	120	59% (10A/g) ~94% (1000 cycles)	

References

1. Y. G. Li, Y. Y. Wu, *J. Am. Chem. Soc.*, 2009, **131**, 5851.
2. N. P. Wickramaratne, J. Xu, M. Wang, L. Zhu, L. Dai and M. Jaroniec, *Chem. Mater.*, 2014, **26**, 2820.
3. M. Sevilla and A. B. Fuyertes, *ACS Nano*, 2014, **8**, 5069.
4. C. Yuan, X. Liu, M. Jia, Z. Luo and J. Yao, *J. Mater. Chem. A*, 2015, **3**, 3409.
5. J. Han, G. Xu, B. Ding, J. Pan, H. Dou, and D. R. MacFarlane, *J. Mater. Chem. A*, 2014, **2**, 5352.
6. T. Yang, R. Zhou, D.-W. Wang, S. P. Jiang, Y. Yamauchi, S. Z. Qiao, M. J. Monteiro and J. Liu, *Chem. Commun.*, 2015, **51**, 2518.
7. H. Wang, L. Shi, T. Yan, J. Zhang, Q. Zhong and D. Zhang, *J. Mater. Chem. A*, 2014, **2**, 4739.
8. S.-K. Kim, E. Jung, M. D. Goodman, K. S. Schweizer, N. Tatsuda, K. Yano and P. V. Braun, *ACS Appl. Mater. Interfaces*, 2015, **7**, 9128.